ANNUAL REVIEWS

Annual Review of Biomedical Engineering

Cuffless Blood Pressure Measurement

Ramakrishna Mukkamala,[1] George S. Stergiou,[2] and Alberto P. Avolio[3]

[1]Department of Bioengineering and Department of Anesthesiology and Perioperative Medicine, University of Pittsburgh, Pittsburgh, Pennsylvania, USA; email: rmukkamala@pitt.edu

[2]Hypertension Center STRIDE-7, School of Medicine, Third Department of Medicine, National and Kapodistrian University of Athens, Sotiria Hospital, Athens, Greece; email: gstergi@med.uoa.gr, stergiougs@gmail.com

[3]Macquarie Medical School, Faculty of Medicine, Health and Human Sciences, Macquarie University, Sydney, New South Wales, Australia; email: alberto.avolio@mq.edu.au

Annu. Rev. Biomed. Eng. 2022. 24:203–30

First published as a Review in Advance on April 1, 2022

The *Annual Review of Biomedical Engineering* is online at bioeng.annualreviews.org

https://doi.org/10.1146/annurev-bioeng-110220-014644

Keywords

blood pressure determination, cuffless blood pressure, oscillometry, pulse transit time, pulse wave analysis, wearable electronic devices

Abstract

Cuffless blood pressure (BP) measurement has become a popular field due to clinical need and technological opportunity. However, no method has been broadly accepted hitherto. The objective of this review is to accelerate progress in the development and application of cuffless BP measurement methods. We begin by describing the principles of conventional BP measurement, outstanding hypertension/hypotension problems that could be addressed with cuffless methods, and recent technological advances, including smartphone proliferation and wearable sensing, that are driving the field. We then present all major cuffless methods under investigation, including their current evidence. Our presentation includes calibrated methods (i.e., pulse transit time, pulse wave analysis, and facial video processing) and uncalibrated methods (i.e., cuffless oscillometry, ultrasound, and volume control). The calibrated methods can offer convenience advantages, whereas the uncalibrated methods do not require periodic cuff device usage or demographic inputs. We conclude by summarizing the field and highlighting potentially useful future research directions.

Contents

1. INTRODUCTION

Cuffless blood pressure (BP) measurement offers great promise for mitigating the burden of hypertension, which is the leading cause of morbidity and mortality worldwide (1), as well as hypotension, which is common and a precursor of mortality following major surgery and in critical care (2–4). The opportunity for such monitoring is as high as ever due to recent technological advances, including the proliferation of smartphones with sensors therein and unobtrusive wearable sensing. For these two reasons, studies on cuffless BP measurement have been increasingly appearing in the literature, and devices are now emerging in the marketplace (5–9). Despite considerable advances, the realization of cuffless BP monitoring has proved difficult, and to date, no device or measurement principle has been widely accepted.

The objective of this review is to accelerate progress in the development and application of cuffless BP measurement methods. As a complement to previous reviews focusing on a particular aspect of the field (10–20), this review covers all major potential principles backed by a useful reference list. We begin by explaining the conventional BP measurement methods. We then argue how eliminating the inflatable cuff from noninvasive BP monitoring would help in addressing profound clinical problems. After describing the technological drivers, we present the major cuffless BP measurement methods under investigation, in terms of high-level concepts, salient details, and supporting evidence. We conclude by summarizing the state of the art and highlighting key future directions.

2. CONVENTIONAL BP MEASUREMENT METHODS

BP is a vital sign and perhaps the most important physiological variable for monitoring. Elevated and low BP are common. Hypertension is a major risk factor for cardiovascular end-organ damage, morbidity, and mortality; usually asymptomatic; and often treatable. Hypotension is an important indicator of inadequate tissue perfusion and likewise modifiable. As shown in **Figure 1**, there are five conventional BP measurement methods (see the sidebar titled Brief History of BP Measurement).

Arterial catheterization is the invasive gold-standard method (22) (see **Figure 1*a***). A manometer is placed in fluid contact with blood in a large artery to measure the BP waveform. A waveform can be analyzed to track other important variables such as cardiac output (23, 24).

BP: blood pressure

Manual auscultation is the standard noninvasive method (25) (see **Figure 1*b***). A stethoscope used by a human observer is positioned over the brachial artery, and an appropriately sized upper

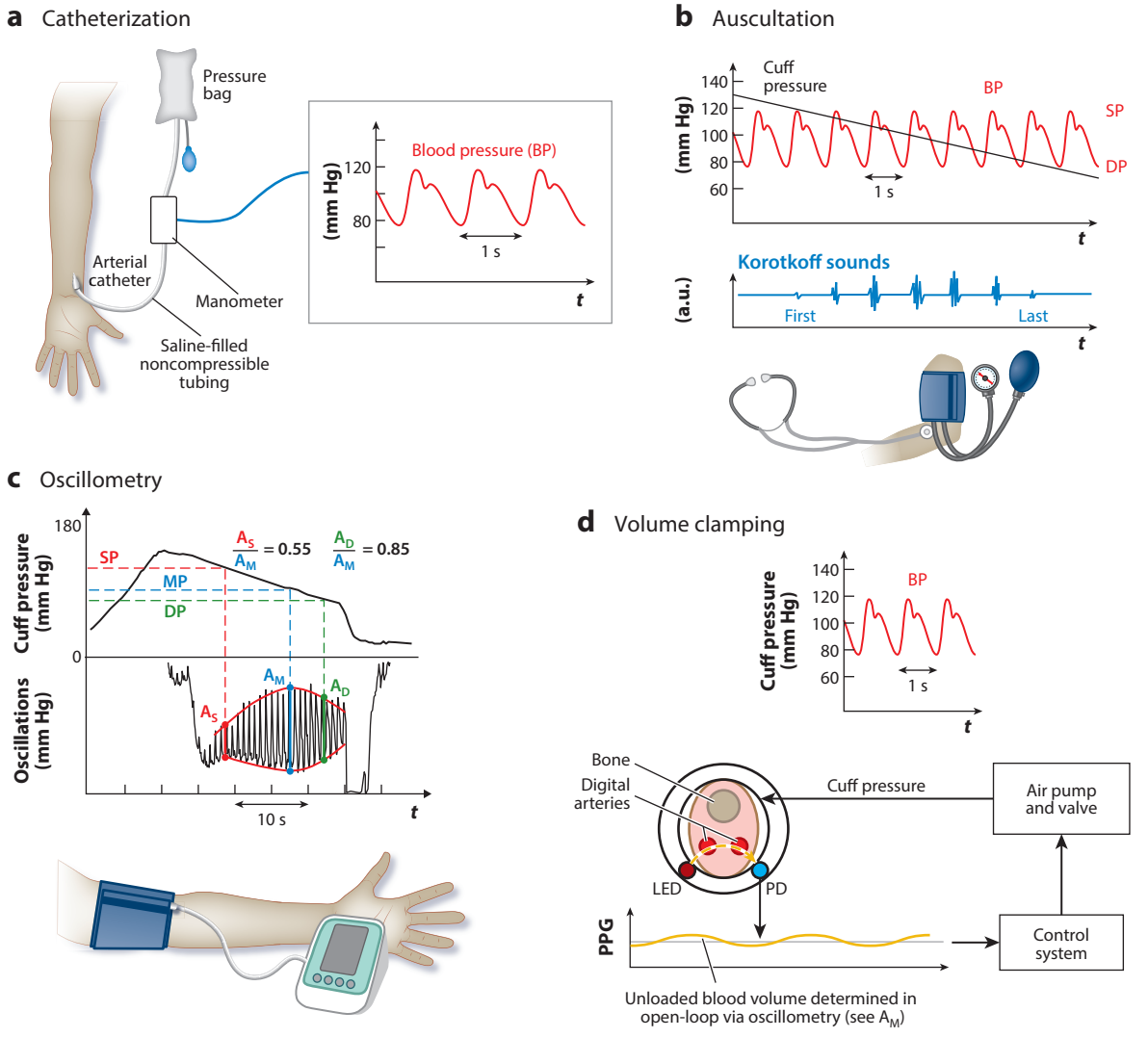

(Caption appears on following page)

Figure 1 (*Figure appears on preceding page*)

Conventional BP measurement methods. Standard or widely used methods include catheterization (*a*), auscultation (*b*), and oscillometry (*c*). Volume clamping (*d*) and tonometry (*e*) are less common methods for noninvasive measurement of the BP waveform. All the noninvasive methods require an inflatable cuff, which is not readily available and cumbersome to use. Abbreviations: A_D, oscillogram amplitude when cuff pressure is at diastolic blood pressure; A_M, maximum oscillogram amplitude; A_S, oscillogram amplitude when cuff pressure is at systolic blood pressure; BP, blood pressure; DP, diastolic BP; F, force; LED, light-emitting diode; MP, mean BP; PD, photodetector; P_i, internal BP; PPG, photoplethysmography; SP, systolic BP; *t*, time; *T*, arterial wall tension.

arm cuff is inflated to occlude blood flow. The observer detects the Korotkoff sounds during slow cuff deflation while monitoring the pressure in the cuff via an external manometer. The first sound (Korotkoff phase I) indicates the initiation of turbulent flow and thus systolic BP (SP), and the silent last sound (Korotkoff phase V) indicates the renewal of laminar flow and thus diastolic BP (DP). Auscultation may also be automated by incorporating a microphone in the cuff (26).

SP: systolic BP

DP: diastolic BP

MP: mean BP

PPG: photoplethysmography

Oscillometry is another noninvasive and automatic method and currently the most widely used in clinical practice (27–30) (see **Figure 1*c***). A cuff placed around the upper arm (or wrist or ankle) is slowly deflated (or inflated) between suprasystolic and subdiastolic cuff pressures while the cuff pressure is recorded. The manometer resides in the monitor rather than the cuff, so precise sensor positioning is not a factor, as it is in auscultation. The cuff pressure indicates the applied pressure and includes small oscillations reflecting the pulsatile arterial blood volume (e.g., arterial dilation compresses the air-filled cuff to increase the cuff pressure). The amplitude of the oscillations varies with the applied pressure, as the arterial blood volume–transmural pressure relationship is nonlinear. (Transmural pressure of an artery is defined as its internal minus external pressures.) BP is computed from the oscillation amplitude versus applied pressure function (i.e., oscillogram) using a population-average algorithm, which is brand and device specific. The standard algorithm is to compute mean BP (MP) as the cuff pressure at which the oscillogram is maximal, as the slope of the blood volume–transmural pressure relationship peaks near zero transmural pressure (see A_M in **Figure 1*c***), and SP and DP as the cuff pressures at which the oscillogram amplitudes are certain fixed ratios of the maximal amplitude (see A_S/A_M and A_D/A_M in **Figure 1*c***).

Volume clamping is a noninvasive and automatic method for measuring a finger BP waveform (31–34) (see **Figure 1*d***). A cuff embedded with a photoplethysmography (PPG) sensor is placed around a finger. The PPG sensor measures the blood volume oscillations in the digital arteries, while a manometer records the cuff pressure. First, the cuff pressure is slowly increased to identify the blood volume at which the artery is unloaded (i.e., zero transmural pressure). The standard algorithm is to take the average of the PPG oscillation of maximal amplitude, which occurs at a cuff

BRIEF HISTORY OF BP MEASUREMENT

Blood pressure (BP) measurement has a history of almost three centuries (21). In 1733, Stephen Hales, an English clergyman, was the first to measure BP and observe its dynamic variation by inserting a glass tube into an artery of a horse. Development of several noninvasive sphygmographs followed. The invention of the sphygmomanometer by Samuel Siegfried Ritter von Basch in 1880, the invention of the pneumatic cuff by Scipione Riva-Rocci in 1896, and the discovery of the Korotkoff sounds by Nikolai Korotkoff in 1905 were milestones in establishing the manual auscultatory cuff BP measurement method. The aneroid auscultatory device importantly followed in 1930. Eventually, in the mid-1970s, the automatic oscillometric cuff BP measurement method, based on a body of earlier work, including the studies of Etienne-Jules Marey in 1881, was introduced. Currently, oscillometry is the recommended method for clinical evaluation of BP in the office, at home, and during 24-h ambulatory monitoring and is the most common method of monitoring BP in surgery and critical care.

pressure near MP according to oscillometry. Then, the cuff pressure is continually varied to clamp the PPG-detected blood volume to its unloaded level throughout the cardiac cycle via a fast servo-control system. The cuff pressure may thus equal the finger BP waveform. The unloaded blood volume varies with changes in vasomotor tone and must be updated frequently for continuous monitoring.

Tonometry is a noninvasive method for measuring a BP waveform from large, superficial arteries (35–37) (see **Figure 1*e***). A force sensor is pressed on the skin overlying the artery. The sensor must (*a*) applanate (i.e., flatten) the artery so that its wall tension, which provides force balance with BP, is perpendicular to the sensor and (*b*) be encompassed by the flattened artery so that BP may be derived as the measured force divided by the known sensor area. An array of small force sensors is employed to ease sensor positioning, and the hold-down force is slowly increased, automatically for the radial artery via a cuff-like device or manually via a hand-held pen device, to identify applanation. The sensor and hold-down force are selected via an algorithm. A basic algorithm detects the largest amplitude pulse, which may correspond to the BP waveform. Maintaining the single hold-down force thereafter may permit continuous monitoring. However, satisfying the two conditions has proved difficult, and the measured waveform is routinely calibrated with cuff BP values in practice.

The noninvasive methods estimate rather than directly measure BP, so their accuracy is a concern. However, much of the epidemiological data on high BP were obtained using manual auscultation (38). Hence, although this method is imperfect and known to underestimate invasive brachial SP and overestimate invasive brachial DP, for example, its accuracy is seldom questioned (39). Many oscillometric devices, some automatic auscultatory devices, and a few volume clamping devices have been validated for accuracy against manual auscultation or catheterization using an established protocol (40, 41). Office, home, and ambulatory devices are validated against auscultation performed by two observers simultaneously in individuals with diverse BP levels and other characteristics, whereas perioperative and critical care devices are often validated against conventional radial artery catheterization in patients with varying BP levels. The devices must satisfy predefined accuracy criteria, including bias and precision errors (i.e., mean and standard deviation of the BP errors) within ± 5 and 8 mm Hg (41). However, it is important to recognize that these errors can be partly attributed to reference measurement errors. Note that DP and MP are similar throughout the larger arteries but lower in the finger and other smaller arteries due to Poiseuille's law relating vessel caliber to vascular resistance, while SP rises with increasing distance from the heart due to arterial wave reflection and stiffening (42). As a result, automatic cuff devices include BP conversion algorithms when their measurement site is different from the reference site to satisfy the error limits (43, 44). For this reason, volume clamping devices, which target finger BP, may be less accurate.

Oscillometric devices are relatively accurate, easiest to use, free of observer bias, and inexpensive. Hence, oscillometry has become the dominant BP measurement method in clinical practice. In fact, most of the large-outcome hypertension trials in the past 20 years that have demonstrated the benefits of treatment-induced BP decline in preventing cardiovascular events and death have used this method (45).

3. THE CASE FOR CUFFLESS BP MEASUREMENT

Common to all the noninvasive BP measurement methods is reliance on an inflatable cuff. The cuff requirement carries three limitations.

The most important limitation is that cuff devices are not readily available. Many people in low-resource settings have no access to these devices, whereas others must go out of their way to use the

ECG: electrocardiography

cumbersome devices. As a result, numerous people do not check their BP as required to be aware of their hypertensive condition or to be motivated enough to take their BP-lowering medications. In fact, only about three in seven hypertensives in the world are aware of their condition, and just one out of these seven has their BP under control (46). Hypertension consequently remains the leading cause of disability-adjusted life years lost worldwide (1).

Another limitation is that repeated cuff inflations and deflations are disruptive to patients undergoing gold-standard hypertension diagnosis via 24-h ambulatory BP monitoring, which overcomes the white coat and masked hypertension effects in the office and large intraperson BP variations (47, 48), or hypotension surveillance following major surgery and in critical care (2–4). The disturbing cuff is an important contributing factor to the marked underutilization of ambulatory BP monitoring (49) and may diminish the clinical value of nighttime BP (50). It is also the reason that cuff BP measurements are made too infrequently (often every 4–8 h) in postsurgical patients who commonly develop hypotension, which is a harbinger of mortality (2). In fact, if the initial month after major surgery were viewed as a disease, it would be the third leading cause of death in the United States (2).

A third limitation is that widely used oscillometric cuff devices do not provide continuous BP measurement. As a result, immediate detection of hypotension and real-time titration of therapy during perioperative and critical care are often not possible, and the dynamic BP response to daily physical and mental activities is unknown.

Eliminating the cuff from noninvasive BP measurement is necessary for addressing the following issues:

1. Hypertension awareness by bringing regular BP monitoring to the masses during daily life
2. Long-term hypertension control by continually monitoring and revealing high BP readings to individual patients (51)
3. Precise hypertension evaluation and diagnosis by affording unobtrusive BP monitoring during the day and night
4. Hypotension surveillance and therapy by providing seamless, continuous BP monitoring

Furthermore, by furnishing unprecedented BP data during all daily circumstances rather than merely providing snapshots of the BP profile (e.g., video versus pictures), the cuffless paradigm could revolutionize hypertension evaluation and management altogether. In these and other ways, cuffless BP measurement can improve the assessment of BP and thereby mitigate the devastating burden of elevated and low BP.

4. TECHNOLOGICAL DRIVERS FOR CUFFLESS BP MEASUREMENT

The opportunity for cuffless BP measurement is being driven by recent technological advances. Fundamental developments including miniaturization, wireless communication, efficient power consumption, and pervasive computing have been integrated to transform conventional cardiovascular sensing from cumbersome to convenient form factors (52).

4.1. Conventional Cardiovascular Sensing

Figure 2*a* illustrates some popular sensing methods for noninvasive measurement of physiological variables related to BP. These and other methods are as follows. Electrocardiography (ECG) measures the cardiac electrical activity initiating mechanical contraction via electrode voltage difference across the heart. This method is most robust to the various noise sources. PPG measures blood volume oscillations conventionally from an extremity by shining light on

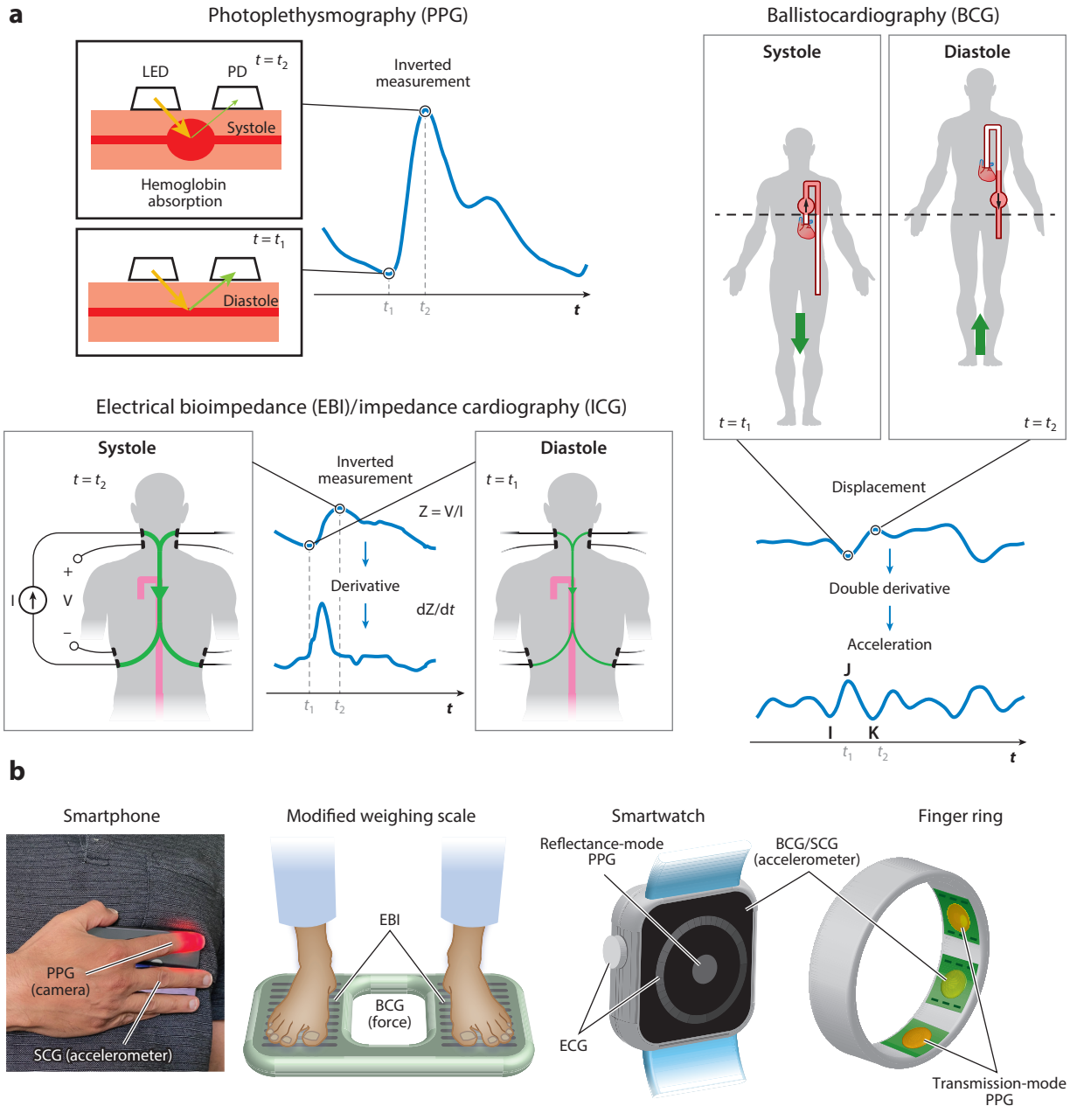

Figure 2

Recent technological advances that are driving the field of cuffless BP measurement. (*a*) Some conventional sensing methods for noninvasive measurement of physiological variables related to BP. (*b*) Some new form factors for convenient implementation of the conventional sensing methods. Shown from left to right: the iPhone X (Apple), PhysioWave Pro (PhysioWave), Apple Watch Series 6 (Apple), and Oura Ring (Oura). Abbreviations: BP, blood pressure; ECG, electrocardiography; I, current; LED, light-emitting diode; PD, photodetector; SCG, seismocardiography; *t*, time; V, voltage; Z, impedance.

EBI: electrical bioimpedance

ICG: impedance cardiography

BCG: ballistocardiography

SCG: seismocardiography

tissue and receiving the transmitted or reflected light, which fluctuates about its mean mainly due to light absorption by hemoglobin in pulsatile arterial blood (53–55) (see **Figure 2*a***). This method may best balance simplicity and effectiveness. Ultrasound measures the absolute blood volume/cross-sectional area and blood velocity waveforms of an artery via M-mode and Doppler principles (56). Unlike PPG, this method can reach deep arteries but requires meticulous probe placement. Electrical bioimpedance (EBI) measures blood volume oscillations by employing electrodes to inject current, usually into the thorax [for impedance cardiography (ICG)], and to derive the resulting electrical impedance, which varies mainly due to highly conductive pulsatile blood (57, 58) (see **Figure 2*a***). This method offers greater penetration depth than PPG and is simpler than ultrasound but does not yield as high-quality waveforms. Ballistocardiography (BCG) measures the reactionary body movements that occur with aortic blood ejection, traditionally via a bed-like table with a mobile top surface and an accelerometer (59, 60) (see **Figure 2*a***). This method is versatile in terms of sensing but susceptible to motion artifact. Seismocardiography (SCG) measures low-frequency cardiac vibrations via a chest motion sensor (59). This method can leverage the same sensor to measure high-frequency vibrations (i.e., phonocardiography), but sensor positioning and motion artifacts are complicating factors.

4.2. Recent, Convenient Form Factors

Figure 2*b* illustrates some of the recent form factors for convenient implementation of the conventional sensing methods. These technological drivers include wearables and so-called nearables.

Smartphones may afford the most important form factor due to their ubiquity and constant usage. The smartphone camera, which is a visible light detector, can measure a reflectance-mode PPG waveform when a user places their fingertip on the camera with the adjacent flash serving as the light source (61) (see **Figure 2*b***) or even without contact by leveraging ambient light for illumination and recording video of a skin region, usually from the face (62). The video may also permit noncontact measurement of the BCG waveform via vertical body movements (63). The smartphone accelerometer may be employed for contact measurement of the BCG waveform by having the user hold the phone against their body or the SCG waveform by having the user position the phone on their chest (64) (see **Figure 2*b***). High-end smartphones include additional transducers, such as an infrared PPG sensor [Galaxy S5 (Samsung)], for deeper penetration and thus robust measurement in low signal conditions (e.g., dark skin, cold-induced vasoconstriction) or a strain gauge array under the screen for sensitive force measurement [iPhone 6s–X (Apple)]. Other nearables include pocket-size electrode pads for on-demand measurement of the ECG waveform [KardiaMobile (AliveCor)], bed force sensors for seamless measurement of the BCG waveform at night [Sleep Monitor (Beddit), Sleep (Withings)], and a modified weighing scale for on-demand but higher-quality measurement of the BCG in the principal head-to-toe direction as well as the foot EBI waveform [PhysioWave Pro (PhysioWave)] (see **Figure 2*b***).

Smartwatches and fitness bands are the most popular wearables and include a PPG sensor to target measurement from cutaneous arteries on the back of the wrist and an accelerometer for potential measurement of BCG and SCG waveforms (65). Some smartwatches also include electrodes for on-demand measurement of the ECG waveform [Apple Watch Series 4 (Apple)] (see **Figure 2*b***). Less common wearables include chest patches for continuous measurement of the ECG, SCG, or PPG waveforms [Zio Patch (iRhythm), BodyGuardian Heart (Preventice)] and a finger ring with an infrared PPG sensor for superior measurement from the larger digital arteries plus an accelerometer [Motiv Ring (Motiv), Oura Ring (Oura)] (see **Figure 2*b***). Soft wearable sensors are being developed that are practically imperceptible and conform to the body for highest fidelity measurement of various arterial waveforms (66–69). However, the circuitry needed for waveform acquisition remains rigid.

These technological advances are drivers in that they could be combined with a cuffless method to address the clinical problems. Incorporating additional sensors or different sensors altogether, data analytics, or actuation-like cuff devices are necessary to measure BP.

PTT: pulse transit time

PWA: pulse wave analysis

5. POTENTIAL CUFFLESS BP MEASUREMENT METHODS

Potential cuffless BP measurement methods may be categorized as calibrated or uncalibrated. Calibrated methods obtain one or more variables that correlate with BP and then map or calibrate the variable(s) to mm Hg units using periodic cuff BP measurements or demographic inputs. Uncalibrated methods do not require either type of calibration but are generally less convenient than calibrated methods (e.g., once the cuff BP measurement for calibration has been obtained).

5.1. Calibrated

There are three major calibrated cuffless BP measurement methods: pulse transit time (PTT), pulse wave analysis (PWA), and facial video processing. Several aspects of especially the first two methods are covered in a recent book (11).

5.1.1. Pulse transit time. PTT may be the only convenient correlate of BP based on robust theoretical principles. The popular method is the subject of recent reviews (10–12, 14, 15, 17) and summarized in **Figure 3**.

The PTT theory is as follows (see **Figure 3*a***). Cardiac ejection initiates a pressure wave that travels through the arteries. This wave may be visualized as acute arterial dilation and moves considerably faster than blood. PTT is the time delay for the pressure wave to travel between proximal and distal arterial sites. It decreases (i.e., faster wave travel) as the artery stiffens due to fluid dynamic principles. This relationship for PTT (τ) in the form of pulse wave velocity ($v = l/\tau$, where l is the wave travel length) is encapsulated by the Bramwell-Hill equation (10, 70) as follows:

$$v = \frac{l}{\tau} = \sqrt{\frac{A}{\rho}\frac{dP}{dA}}. \quad 1.$$

Here, A is the cross-sectional area of the artery, P is BP, ρ is blood density, and dA/dP is the arterial compliance. The ratio of arterial compliance to area denotes distensibility, which is an inverse, relative metric of arterial stiffness. Distensibility decreases with increasing BP (and vice versa) due to the material properties of the arterial wall. This relationship for the aorta is captured by the Wesseling model (23) as follows:

$$\frac{dA/A}{dP} = \left(\pi P_R\left[1 + \left(\frac{P - P_M}{P_R}\right)^2\right]\left[\frac{1}{2} + \frac{1}{\pi}\tan^{-1}\left(\frac{P - P_M}{P_R}\right)\right]\right)^{-1}. \quad 2.$$

Here, P_M and P_R indicate the slope and width of the approximate linear regime of the sigmoidal arterial $A - P$ function. Combining these equations while assuming higher BP ($P \gg P_M + P_R$) yields the following inverse BP-PTT relationship:

$$P = K_1\frac{1}{\tau} + K_2, \quad 3.$$

where $K_1 = l\sqrt{\frac{2\rho P_R}{\pi+2}}$ and $K_2 = P_M$ are positive, person-specific parameters (71).

Equation 3 is not generally valid. Distensibility and thus PTT can change independently of BP via arterial smooth muscle contraction and aging-induced arteriosclerosis [which cause K_1 and K_2 to decline over time (23)]. However, smooth muscle, whose contraction varies on timescales of

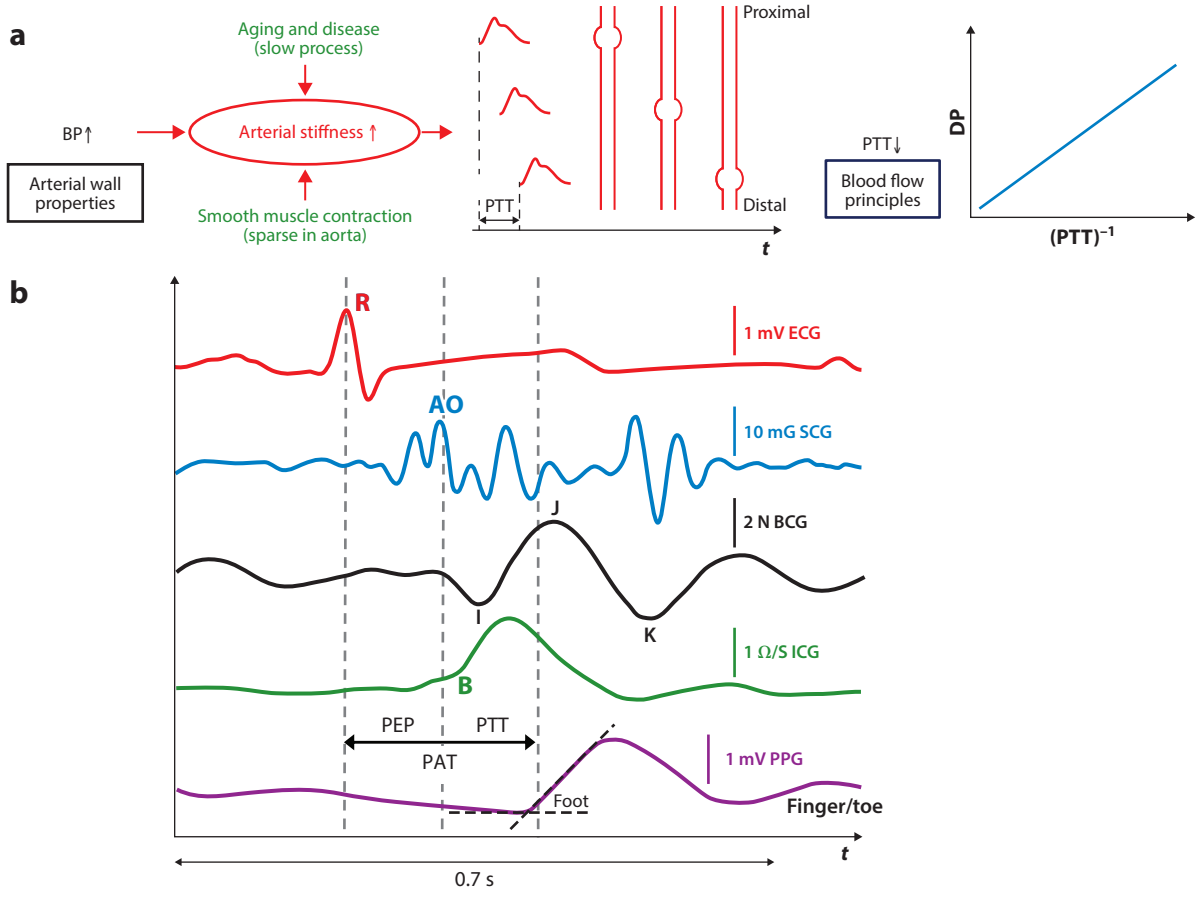

(*Caption appears on following page*)

Figure 3 (*Figure appears on preceding page*)

PTT method for calibrated, cuffless BP measurement. (*a*) Theoretical basis. Panel adapted from Reference 14. (*b*) Detection of PTT or PAT surrogate from two cardiovascular waveforms (see **Figure 2**). Panel adapted from Reference 59. (*c*) Calibration of the time delay (τ, ms) to BP (P, mm Hg). K_i are parameters of a calibration model that are determined via cuff BP measurements in one of three ways. Panel adapted from Reference 14. Abbreviations: BCG, ballistocardiography; BP, blood pressure; DP, diastolic BP; ECG, electrocardiography; ICG, impedance cardiography; PAT, pulse arrival time; PEP, pre-ejection period; PPG, photoplethysmography; PTT, pulse transit time; SCG, seismocardiography.

seconds to minutes due to neurohumoral control mechanisms, is less abundant in the aorta, and vascular aging is a slow process. Consequently, Equation 3 is most tenable for aortic PTT over time periods of six months or more, in which aging is not a contributing factor (72).

PTT can be measured simply as the time delay between proximal and distal arterial waveforms. Conventionally, for studies of arterial stiffness, PTT is detected as the foot-to-foot time delay between BP waveforms (42). The reason is that the foot occurs early in systole before the pressure wave, which is reflected mainly at the arterioles, returns to the heart. Since the waveform feet are at the level of diastole, conventional PTT tracks DP.

This theory is substantiated by animal studies. Aortic PTT detected invasively or even noninvasively via PPG shows remarkable intrasubject correlation with DP (10, 73).

PTT measurement is as follows (see **Figure 3*b***). In humans, aortic PTT measurement involves acquiring arterial waveforms from the carotid and femoral arteries or employing ultrasound and is relatively difficult. As a result, approximations to the theory are made. In fact, ECG is most often used to obtain a surrogate of the proximal waveform. The time delay between the R-wave of the ECG waveform and some fiducial marker of an arterial waveform is called pulse arrival time (PAT). PAT is the pre-ejection period (PEP) plus the PTT from the aortic root to the arterial waveform measurement site. PEP depends on ventricular properties, so it can change independently of PTT and BP and quickly (10, 73). Due to this dependency, PAT shows better correlation with SP than with DP. Finger PPG is most commonly used to obtain the distal waveform. Popular finger PAT is thus susceptible to smooth muscle contraction in the arm and PEP. The I-wave of the BCG waveform (see Section 5.1.2), AO point of the SCG waveform (59), and B point of the ICG waveform (57, 58) may indicate aortic valve opening but at the cost of robustness and convenience. Ear PPG may be another option for eliminating PEP but does not indicate the true proximal timing. Toe PPG offers an alternative distal waveform for detecting PTT through the aorta and legs but is less convenient than finger PPG. The best fiducial marker for a PPG waveform is its foot, which is well detected with the intersecting tangent method (74). The foot location does, however, depend on the contact pressure applied by the PPG sensor (75).

PTT calibration is described in a recent book chapter (76) and summarized as follows (see **Figure 3*c***). A parametric model serves to convert the time delay in units of milliseconds to BP in units of mm Hg. Equation 3 is an effective model. Simultaneous measurements of the time delay and cuff BP are obtained to determine the multiple model parameters for an individual. Cuffless BP may then be obtained for that individual by applying the detected time delay to the fully defined calibration model. The parameters must be updated periodically (e.g., every few months) to account for vascular aging (72). By leveraging the fact that SP and DP often show correlations of 0.7–0.8 (77, 78), two calibration models are sometimes built to map the single time delay to each BP level.

PAT: pulse arrival time

PEP: pre-ejection period

The model parameters are determined via a person-specific, population-based, or hybrid method. In the person-specific method, all model parameters are determined from simultaneous measurements of the time delay and cuff BP from the individual during interventions that change BP (76). A hydrostatic maneuver is not an obvious intervention, yet it is practical and effective.

This maneuver is performed by varying the vertical height (h) of the effective BP measurement site relative to the heart (79, 80). Due to the weight of the blood column, the maneuver will cause the local BP to change by $\rho g h$, where ρ is again the density of blood and near that of water, g is gravity, and h is measured (via, e.g., an accelerometer). A change in h of just 10 cm will cause BP to change by over 7 mm Hg. For example, in the case of finger PAT, fully lowering/raising the hand from heart level may increase/decrease the BP effectively obtained from the midpoint of the arm by about 25 mm Hg for an average arm length. In the population-based method, all model parameters for an individual are determined using a training dataset comprising measurement pairs of the time delay and cuff BP from a cohort of different individuals. The parameters must be functions of basic demographic information such as age and sex (81). In the hybrid method, one parameter (usually K_2 in Equation 3) is determined from a single time delay and cuff BP measurement pair, and the remaining parameter is determined from demographic information and a similar training dataset. The hybrid and person-specific methods must be applied periodically to account for aging (i.e., cuff recalibrations), while the population-based method is essentially calibration-free from the user's perspective. Overall, the hybrid method balances accuracy and convenience.

Evidence for the PTT method is summarized as follows. Finger PAT has been investigated the most by far. It is useful in tracking SP during exercise (10). However, **Table 1** provides a summary of some challenging evaluation studies of finger PAT and other time delays (82–89). The correlation between finger PAT and SP may generally be about only −0.5. There is conflicting or little evidence on the benefit of using ear PPG, ICG, BCG, or SCG to obtain the proximal waveform. By contrast, using toe PPG to obtain the distal waveform does appear to improve the correlation with BP. Nevertheless, finger PAT is more practical than other time delays and could take on several convenient form factors (e.g., smartwatch for on-demand BP measurement; see **Figure 2*b***). There is now a wearable finger PAT-based device for hospital use [ViSi Mobile System (Sotera Wireless)] (5). This device has had US Food and Drug Administration (FDA) clearance for the past several years. The device includes an automatic upper-arm cuff BP measurement device for calibration, which is performed with every detected significant change in MP. However, published results on device accuracy between the cuff calibrations may be limited. Overall, while calibration of PTT or any other BP correlate is often considered the major hurdle, practical PTT measurements have yet to convincingly show high intraindividual correlations with BP.

5.1.2. Pulse wave analysis. PWA involves extracting features from an arterial waveform and mapping them to BP units via a calibration model. This method is more convenient than the PTT method in that only a single sensor is required or may be used with PTT to seamlessly improve its accuracy (see **Figure 3*c***), including via independent tracking of SP and DP. Because of these advantages and the popularity of machine learning, the PWA method is garnering increasing attention.

PWA is most often performed on a PPG waveform, as summarized in recent reviews and shown in **Figure 4*a*** (11, 14, 16, 18, 20). However, this PWA may not have solid theoretical underpinnings. Unlike large, elastic arteries, the small arteries interrogated by PPG are viscoelastic (10). The Kelvin-Voigt model of viscoelasticity provides the following relationship between the Fourier transforms of the AC components of the PPG waveform [$\Delta V(\omega)$] and BP waveform [$\Delta P(\omega)$]:

$$\Delta V(\omega) = \frac{1}{j\omega\eta + E}\Delta P(\omega), \qquad 4.$$

where E and η are, respectively, the elastic modulus and coefficient of viscosity of the arterial wall (90). The model transfer function is a low-pass filter with $1/E$ gain and E/η cutoff frequency. The PPG waveform is thus a low-pass filtered version of the BP waveform at the same arterial site.

Table 1 Summary of challenging evaluation studies on the PTT method[a]

Study participants	Number of participants	BP interventions	Reference BP device	PTT detection	Results			Reference
					SP	MP	DP	
Evaluation method: no calibration; intraindividual correlation coefficient								
Young and healthy	12	Nitroglycerin Angiotensin II Norepinephrine Salbutamol	Arterial catheter	ECG (R-wave) Finger PPG (foot)	−0.62	−0.28	−0.14	82
				ICG (B-point) Finger PPG (foot)	−0.57	−0.67	−0.64	
ICU	121	Clinical	Arterial catheter	ECG (R-wave) Finger PPG (foot)	−0.41	−0.30	−0.20	83
ICU	23	Clinical	Arterial catheter	ECG (R-wave) Finger PPG (foot)	−0.52	−0.48	−0.39	84
Normotensive	58	Spinal anesthesia	Automatic arm cuff	ECG (R-wave) Toe PPG (foot)	NR	−0.74	NR	85
Pregnancy-induced hypertension	15					−0.67		
Surgery	2,309	Clinical	Arterial catheter	ECG (R-wave) Finger PPG (foot)	−0.37	−0.34	−0.30	86
Young and healthy	22	Mental arithmetic Cold pressor Stair climbing	Volume clamping finger cuff	BCG (I-wave) Toe PPG (foot)	−0.70	NR	−0.70	87
				ECG (R-wave) Finger PPG (foot)	−0.70	NR	−0.55	
Normotensive and hypertensive	32	Slow breathing Mental arithmetic Cold pressor Sublingual nitroglycerin	Manual cuff	ECG (R-wave) Toe PPG (foot)	−0.63	NR	−0.33	88
				ECG (R-wave) Ear PPG (foot)	−0.24		−0.19	
				ECG (R-wave) Finger PPG (foot)	−0.42		−0.28	
				Ear PPG (foot) Toe PPG (foot)	−0.36		−0.17	
				Ear PPG (foot) Finger PPG (foot)	−0.29		−0.22	
				Finger PPG (foot) Toe PPG (foot)	−0.07		0.05	
Young and healthy	22	Cold pressor Handgrip Cycling	Volume clamping finger cuff	SCG (AO point) Ear PPG (foot)	−0.31	NR	−0.29	89
				SCG (AO point) Forehead PPG (foot)	−0.36		−0.32	
				SCG (AO point) Finger PPG (foot)	−0.39		−0.33	
				ECG (R-wave) Ear PPG (foot)	−0.47		−0.30	
				ECG (R-wave) Forehead PPG (foot)	−0.50		−0.35	
				ECG (R-wave) Finger PPG (foot)	−0.53		−0.36	
Evaluation method: population-based calibration of exponential model; BP error								
Surgery (young and old)	23	Clinical	Arterial catheter	Ear PPG (foot) Toe PPG (foot)	NR	NR	1.4 ± 7.5 mm Hg	81

[a]Table expanded from Reference 14.

Abbreviations: BCG, ballistocardiography; BP, blood pressure; DP, diastolic BP; ECG, electrocardiography; ICG, impedance cardiography; ICU, intensive care unit; MP, mean BP; NR, not reported; PPG, photoplethysmography; PTT, pulse transit time; SCG, seismocardiography; SP, systolic BP.

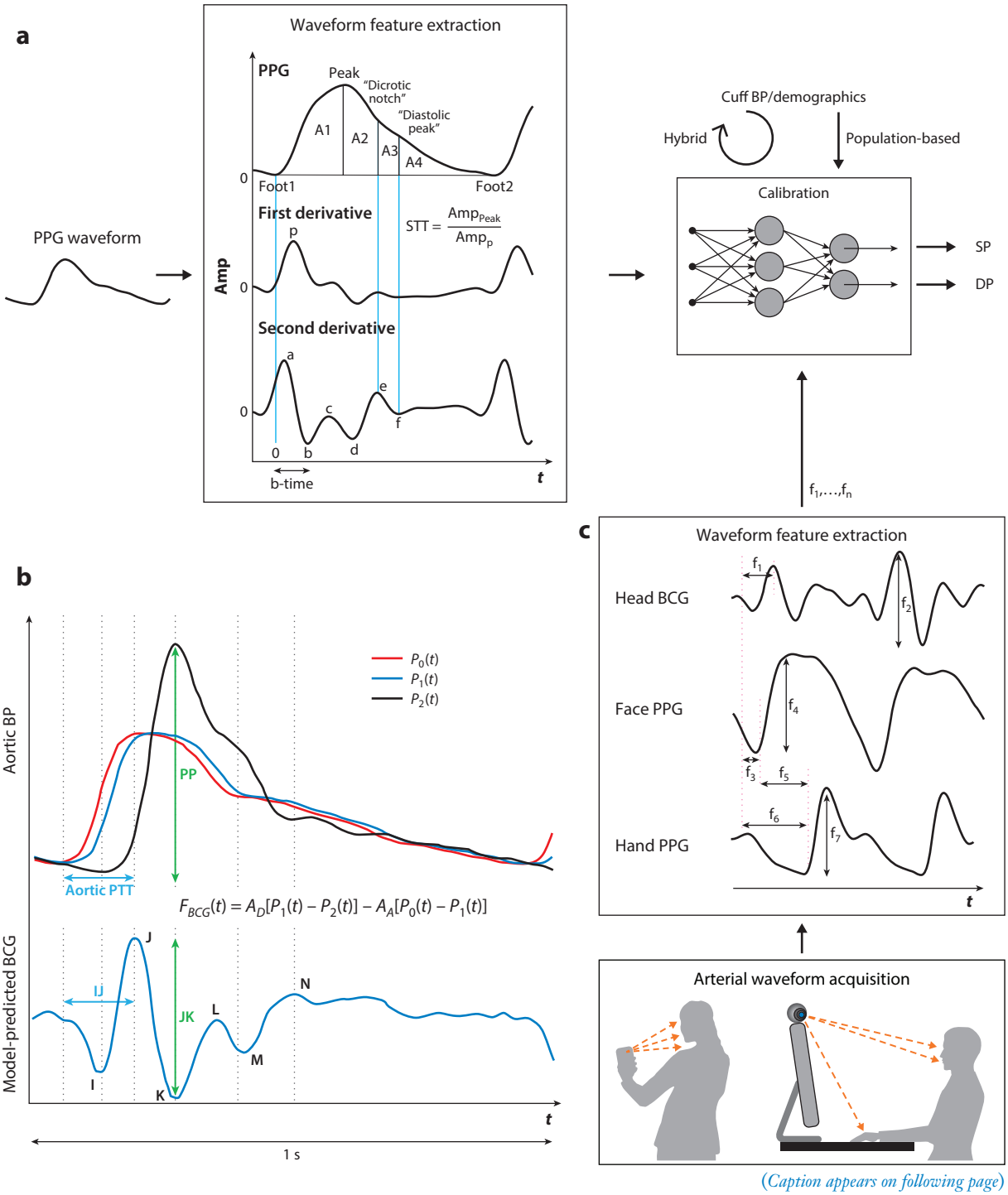

(Caption appears on following page)

Figure 4 (*Figure appears on preceding page*)

Calibrated, cuffless BP measurement methods of greater convenience. (*a*) Popular, data-driven PWA method applied to a single PPG waveform (see **Figure 3*c***for calibration). Panel adapted from Reference 91. (*b*) Model-based PWA method applied to the BCG waveform. $F_{BCG}(t)$ represents the force BCG waveform; $P_0(t)$, $P_1(t)$, and $P_2(t)$ represent BP waveforms at the ascending aortic inlet, aortic arch, and descending aortic outlet; and A_A and A_D are the average cross-sectional areas of the ascending and descending aorta. Panel adapted from Reference 60. (*c*) Facial video processing method for noncontact BP monitoring. Panel adapted from Reference 13. Abbreviations: BCG, ballistocardiography; BP, blood pressure; DP, diastolic BP; PP, pulse pressure; PPG, photoplethysmography; PTT, pulse transit time; PWA, pulse wave analysis; SP, systolic BP; STT, slope transit time.

However, the filter gain and cutoff frequency constantly vary with transmural pressure and smooth muscle contraction, which again can change rapidly and independently of BP. So, for example, the PPG amplitude increases with increasing BP via mental arithmetic [which increases the amplitude of $\Delta P(\omega)$ via stroke volume] but decreases with similar BP increases via a cold pressor test (which increases E via smooth muscle contraction) (91).

Data-driven extraction of features from the PPG waveform should be performed after normalizing its AC component by the DC component to mitigate the impact of variations in lighting, temperature, and skin pigmentation. Moreover, due to the oscillometric principle, the PPG sensor contact pressure impacts the waveform amplitude and shape more than the foot location (75, 91, 92) and should be controlled during the measurement. Numerous features, from simple to complicated, have been explored. Popular ones include derivative-based features, such as the b-time (time from foot to minimum double derivative) (93); slope transit time (STT) (ratio of amplitude to maximum derivative) (94) and time interval between the systolic and diastolic peaks (95), both of which may reflect PTT; and pulse rate and its variability (see **Figure 4*a***).

Calibrating the features to BP is conceptually similar to the PTT method, but there are differences (see **Figure 4*a***). One difference is that multiple features are utilized so that the calibration models include more parameters. The models are often further complicated by accounting for nonlinearities, especially via neural nets. Another difference is that the number of features must also be determined via a separate validation dataset or minimization of a metric that penalizes for number of parameters. The person-specific method, which is intended for determining a small, fixed number of model parameters, is usually not applicable. Hybrid and population-based methods are instead applied. Cuff recalibrations are required for the former.

The number of experimental investigations on PPG waveform analysis is rising. However, the BP variations are often not large, and demographic information is also used to predict BP, which makes interpretation on the added value of the method difficult (96). A few studies suggest that finger PPG waveform analysis can reduce the BP error by about 10% compared to baseline BP prediction models, in which PPG waveform features are excluded as input (91, 97, 98). The useful features are often unclear. One study did reveal that finger b-time and ear STT (see **Figure 4*a***), which reflect PPG fast upstroke intervals, are positively (rather than negatively) correlated with intraindividual SP changes when used along with a PAT (91), whereas another study illustrated the importance of demographic information (99). Interestingly, one study showed that analysis of wrist PPG and accelerometer waveforms could track nocturnal BP dipping but did not disclose the relevant features (100). Despite the paucity of compelling, published data, at least three PPG waveform analysis devices have recently gained some regulatory approval. One device [BB-613 WP (Biobeat Technologies)] comes in the form of a wristband or chest patch, extracts a time delay, and is intended for spot-checking following calibration with an automatic cuff device (6). Another device [Bracelet G1 (Aktiia)] is in the form of a wristband, can be used for frequent monitoring (e.g., 70+ measurements/week), and comes with an automatic arm cuff for recalibration at least every month (7). A third device [Health Monitor/Galaxy Watch Active2 (Samsung)] comes in the form of a wristwatch, must be calibrated with a traditional arm cuff device every 4 weeks, and

PP: pulse pressure

measures BP with a tap on the screen (8). It should also be mentioned that one of the earliest cuffless devices with FDA clearance appears to be based on a similar PWA but applied to a radial artery tonometry waveform [BPro (HealthSTATS)] (9). The device includes a monitor for the back of the wrist, a hemispheric plunger to provide constant pressure on the artery, and a force sensor. Once calibrated with an arm cuff device, the wrist device can measure SP and DP over a 24-h period. Wrist BP changes due to hydrostatic effects may be a challenge for some of these devices.

BCG waveform analysis is a PWA that is far less popular but may have a theoretical basis (see **Figure 4*b***). A mathematical model of the BCG waveform is as follows:

$$F_{BCG}(t) = A_D[P_1(t) - P_2(t)] - A_A[P_0(t) - P_1(t)], \quad 5.$$

where $F_{BCG}(t)$ is the force BCG waveform; $P_0(t)$, $P_1(t)$, and $P_2(t)$ are BP waveforms at the ascending aortic inlet, aortic arch, and descending aortic outlet; and A_A and A_D are the average cross-sectional areas of the ascending and descending aorta (60). This model can predict the major I, J, and K waves in BCG waveforms. Hence, the BCG waves may arise as the difference in BP gradients in the ascending and descending aorta. The model suggests that the IJ time interval may approximately correspond to aortic PTT, while the JK amplitude may be roughly proportional to distal aortic pulse pressure (PP). These two features, as obtained with a force plate and then calibrated with cuff BP values, showed intraindividual correlation with DP and SP of 0.65 on average, which was similar to finger PAT (87). However, additional features may be exploited to better extract aortic PTT and PP from the BCG waveform.

5.1.3. Facial video processing. Noncontact monitoring of BP with a camera generally involves extracting arterial waveform features from facial video and converting them to mm Hg units via a calibration model. While the PWA method requires user activity (e.g., placing a fingertip on a camera) or a special device (e.g., wristband), the noncontact method could permit passive BP monitoring with a ubiquitous device. For example, each time a person uses their smartphone, an application could control the front camera to identify periods in which the user is still and in good lighting to measure BP via facial video processing (101). This increasingly studied, data-driven method is the subject of a recent book chapter (13) and summarized in **Figure 4*c***.

Some key aspects of video processing for extracting arterial waveforms are as follows. For the PPG waveform, a skin region of interest is identified via an existing face detector (102) and spatially averaged per frame to produce red, green, and blue signals. The green signal provides the largest pulse due to the wavelength-dependent light absorption characteristics of hemoglobin, but integrating the signals improves PPG waveform quality by eliminating common artifacts (103). For the BCG waveform, a region of interest representing a boundary such as the shoulder or mouth is identified, available motion estimation methods (104) are applied to track vertical displacements in successive frames of the pixels therein, and the local motion signals are combined. The twice-differentiated signal is a conventional acceleration BCG waveform (see **Figure 2*a***). The blue signal is preferable, because noncontact BCG measures specular reflection rather than the diffuse skin reflection measured by PPG. Postprocessing of the PPG and BCG waveforms is necessary to mitigate nonpulsatile components but not enough to afford signal quality near that of contact sensors.

However, facial video offers spatial and other information not provided by contact sensing. BP-related features in facial video include PTT between proximal and distal facial regions and the face and hand when in the field of view (105), features of the PPG waveform from multiple regions, and BCG waveform features (see **Figure 4**). Facial video also includes possibly useful contextual information such as facial expression, time of day, and setting.

Like the popular PWA method, many features including demographic information are often used. So, calibration of the features to BP is performed analogously to the PWA method.

An increasing number of studies are appearing in the literature. These studies mainly focus on noncontact PPG for tracking BP in controlled conditions (13). However, the studies typically comprise only a few participants with few or no intraindividual BP changes. One study stands out (106). A smartphone camera on a tripod with external light sources was used to extract noncontact PPG waveforms at various facial locations from >1,300 normotensive, East Asian individuals. A neural net with population-based calibration was developed and independently tested using these data with volume clamping finger cuff BP as a reference. This method measured SP better than a model with demographics and pulse rate as input (precision error of 7.3 ± 0.02 versus 8.9 ± 0.0 mm Hg). There is great scope for improving the noncontact method. However, PTT between face and hand PPG waveforms may not be promising, as PTT detected via ear and finger PPG clips may not correlate well with BP (88). Moreover, any improvement may be offset by a diverse participant cohort and intraindividual BP changes. Noncontact BP tracking in uncontrolled settings does not seem realistic.

Noncontact monitoring of BP via arterial vessel image processing could also be feasible. For example, although BP is determined by both the cross-sectional area and variable area-BP relationship of the artery, arterial dimensions and BP may still show positive correlation. One study showed that retinal fundus images, which allow visualization of blood vessels, can be processed to estimate BP (107). A deep learning method was developed and independently tested using these images and reference cuff BP from about 60,000 participants. This method measured SP better than a baseline model that did not include the image as input (absolute error of 11.4 versus 14.6 mm Hg). However, retinal fundus imaging requires sophisticated equipment.

5.2. Uncalibrated

There are at least three uncalibrated cuffless BP measurement methods: cuffless oscillometry, ultrasound, and volume control. These methods do not mandate periodic cuff device usage or demographic inputs.

5.2.1. Cuffless oscillometry. Cuffless oscillometry involves varying the transmural pressure of an artery without an inflatable cuff, using force and PPG sensors to measure the pressure variations and variable-amplitude blood volume oscillations, and computing BP from the oscillogram. The method is described in a recent book chapter (14).

Cuffless oscillometry has been proposed through unique variation of the internal rather than external pressure of an artery (108). A finger ring was built for arm actuation. As the wearer of the ring lowers their hand with arm straight, the internal finger BP rises due to hydrostatic effects. As implied earlier, the BP swing is typically about ±50 mm Hg relative to heart level. For an MP of 90 mm Hg, the transmural pressure ranges from 40 to 140 mm Hg, which corresponds to the left tail of the oscillogram. However, the oscillogram around zero transmural pressure is needed for an inverted U-shape to compute BP. So, the ring must be worn tightly. The device includes an infrared PPG sensor to measure the blood volume oscillations from the digital arteries, a force sensor of known area to measure the PPG sensor contact pressure, and an accelerometer to measure the hydrostatic BP change (i.e., $\rho dg \sin\theta$, where d is the measured arm length and θ is the angle between the arm and horizontal plane obtained via the accelerometer). The PPG sensor contact pressure is subtracted from the hydrostatic BP change to establish the oscillogram abscissa. The main problem is that the PPG sensor contact pressure should be roughly equal to MP, which is what is sought for measurement.

As shown in **Figure 5*a***, finger actuation with a smartphone may be a more practical method to achieve cuffless oscillometry (109). The user presses their fingertip against the phone held at heart level to slowly vary the external pressure of the underlying transverse palmar arch artery. The phone, which includes a PPG force sensor unit, measures the variable-amplitude blood volume oscillations and external pressure, provides feedback to guide the amount of finger pressure over time, and computes BP from the oscillogram. This oscillometric finger pressing method has been implemented as a custom case affixed to the back of a smartphone (109). The case houses an infrared PPG sensor on top of a thin-filmed capacitive force transducer to measure finger pressure only over the known PPG sensor area. The phone includes an application to visually guide the finger actuation and compute SP and DP at the brachial artery from the finger measurements via an empirical algorithm. This method has also been realized as a standalone application that leverages existing sensors in an iPhone (110). The iPhone X application uses the front camera as the PPG sensor and the sensitive strain gauge array under the nearby screen as the force sensor and similarly guides the finger actuation and computes brachial BP. The application includes a one-time measurement of the user's fingertip dimensions to guide finger placement on the screen when measuring BP and estimate the finger contact area on the screen to derive finger pressure. The two devices have been tested in normotensive participants. The custom device was easy to use and yielded BP errors against an automatic arm cuff device that were similar to a volume clamping finger cuff device. The standalone application was not quite as usable and accurate.

Accurate oscillometric BP computation across the clinical BP range constitutes a major hurdle. Mathematical models of the oscillogram may be helpful (28, 111). For example, a model may be employed to compute finger BP from the oscillogram via a person-specific (rather than population-based) algorithm in which the arterial blood volume–transmural pressure relationship is also computed (112, 113). Volume clamping devices may shed light on accurate algorithms for converting the finger BP to brachial BP. These devices use empirical regressions and transfer functions to account for the resistive BP drop and wave reflection (44).

The external pressure of the transverse palmar arch artery may be automatically varied using a nonpneumatic actuator (114). However, note that a new automatic oscillometric device in a wristwatch form factor [HeartGuide (Omron Healthcare)] employs a miniature inflatable cuff and is thus not cuffless (115). While such automatic devices are easier to use, having the user serve as the actuator simplifies the hardware to reach more people (e.g., smartphones are far more ubiquitous than cuff or other specialized devices).

5.2.2. Ultrasound. Ultrasound may afford the only method for uncalibrated measurement of a BP value without variable pressure application. The theory (116) arises by integrating the Bramwell-Hill equation shown in Equation 1 over the cardiac cycle to yield the following relationship:

$$PP = P_s - P_d = \rho \upsilon^2 \ln \frac{A_s}{A_d}, \qquad 6.$$

where A_s and A_d are the absolute cross-sectional areas of an artery at systole and diastole and υ represents the local pulse wave velocity. While υ generally varies throughout the heartbeat (117), it is assumed to be constant here. In this way, cuffless PP may be determined from the known ρ and measurements of an arterial area waveform and pulse wave velocity. Ultrasound may be applied to measure area and blood velocity waveforms. Combining Equation 1 with the Waterhammer equation ($dP/dQ = \sqrt{\rho dP/AdA}$, where Q is the product of area and blood velocity and thus blood volume flow rate) indicates that υ may be computed as the slope of the blood flow rate waveform versus area waveform during early systole wherein wave reflection is minimal

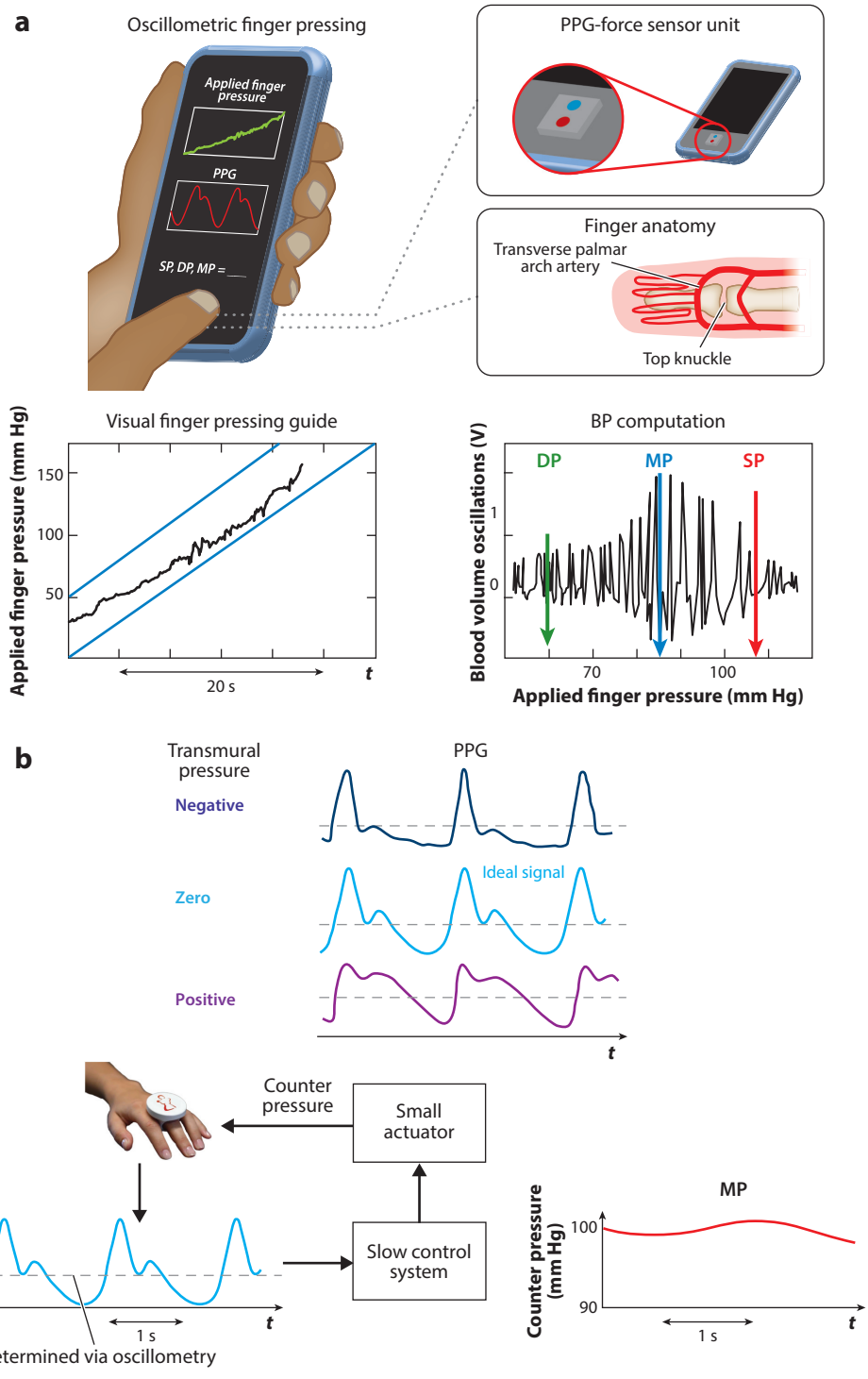

Figure 5

Uncalibrated BP measurement methods based on variable pressure application to an artery without using an inflatable cuff. (*a*) Finger pressing method based on oscillometry (see **Figure 1*c***) for on-demand measurement of BP via a smartphone. Panel adapted from Reference 109. (*b*) Volume control method based on volume clamping (see **Figure 1*d***) for continuous measurement of MP via a finger ring. Panel adapted from Reference 92. Abbreviations: BP, blood pressure; DP, diastolic BP; MP, mean BP; PPG, photoplethysmography; SP, systolic BP.

(flow-area technique) (116, 118). Alternatively, υ may be detected via the time delay between nearby proximal and distal waveforms via ultrasound (119) or another sensor (120). This method may be applied to the aorta or carotid artery and thereby allows measurement of central PP, which is increasingly considered to be of greater clinical value than brachial PP (121). This method has been demonstrated in phantom models and against cuff BP in healthy humans (116, 118–120). However, measurement of SP and DP requires the aid of cuff BP measurements (122, 123).

Combining ultrasound with variable pressure application can permit direct measurement of SP and DP. The principle is similar to oscillometry except that the absolute arterial area or volume is measured, which may help improve accuracy (124). A method was proposed in which a user presses an ultrasound-force probe against the carotid artery but without occluding it via visual guidance, and BP is computed based on a model (125). However, the challenge of any ultrasound method is to offer some convenience advantage over automatic cuff devices.

5.2.3. Volume control. Volume control may be the only uncalibrated method for continuous monitoring of a BP value (92). **Figure 5*b*** illustrates this method. This recent method stems from volume clamping. In this conventional method, clamping the PPG waveform throughout the cardiac cycle allows measurement of the BP waveform but requires fast actuation and thus bulky pneumatic equipment. In the new method, the average of the PPG waveform over the cardiac cycle is clamped to measure the slower changes in MP with, potentially, a small, cuffless device. The contact pressure of the PPG sensor is first increased slowly to compute oscillometric MP. The contact pressure is then set to this value so that the integral of the high-pass filtered PPG waveform (inverted as shown in **Figure 5*b***) over each beat is zero. This integral increases/decreases as the waveform becomes rounder/spikier with positive/negative transmural pressure and thereby serves as the signal for feedback control of the contact pressure. This method, which includes additional control elements, was convincingly demonstrated using volume clamping finger cuff instrumentation against invasive BP in surgical patients, and a finger ring for implementing oscillometry without an inflatable cuff was built. However, this method involves continual application of pressure to the finger equal to the MP, which is not tolerable long-term.

6. CONCLUSIONS

Cuffless BP measurement has become a popular field due to clinical need and technological opportunity. As summarized in **Table 2**, calibrated and uncalibrated methods have been proposed, usually in convenient form factors. Calibrated methods measure correlates of BP, including practical PTTs and contact and noncontact PPG waveform features. These correlates likely track BP variations in a person much better than among groups of people. The methods convert or calibrate the correlates to BP either using periodic cuff BP measurements from the individual or using the individual's demographic data, which are more convenient but less reliable for calibration. While these methods have been extensively studied and cuff-calibrated devices are now on the market, there is no compelling proof in the public domain indicating that they can accurately track intraindividual BP changes. Uncalibrated methods afford BP measurement without using a cuff device or demographic inputs via a solid theory. Although these methods may not generally be as convenient as calibrated methods (e.g., once the cuff calibration has been performed), they can offer convenience or accuracy advantages over automatic cuff devices. Since uncalibrated methods are newer, a body of evidence is lacking. Hence, no cuffless method has yet been broadly accepted.

Our recommendations for future research are as follows:

- Methods: Development of seamless sensors to detect aortic PTT may allow this method to reach its potential. Discovery of features of the PPG and other waveforms that correlate

Table 2 Summary of potential cuffless BP measurement methods

Category	Method	Advantages		Disadvantages		Evidence
Calibrated	PTT	Continuous or passive Seamless	Supporting theory	Periodic cuff calibrations or demographics calibration	Two measurement sites	Many published studies Regulatory-approved, cuff-calibrated, contact devices Limited published data on intraindividual BP change tracking
	PWA (PPG)		Single sensor		Little theory	
	Facial video processing		Ubiquitous device		Little theory Low waveform quality	
Uncalibrated	Cuffless oscillometry (finger pressing)	Calibration-free Solid theory	Potentially ubiquitous device	User activity		Few published studies
	Ultrasound (area-blood velocity)		Central PP measurement	Difficult probe placement		
	Volume control		Continuous	Disruptive (finger numbness)		

Abbreviations: BP, blood pressure; PP, pulse pressure; PPG, photoplethysmography; PTT, pulse transit time; PWA, pulse wave analysis.

with BP in a way that is underpinned by plausible physiological mechanisms is vital for attaining convenience and trust. Creation of an oscillometric finger ring for calibration-free BP measurement may be less disruptive than larger, wrist cuff devices. Development of accurate oscillometric algorithms is also important.

- Data: Building comprehensive training databases is required for deep learning. Such databases may be relatively straightforward to construct for unstable, catheterized patients (126). However, databases for hypertension applications may necessitate test and reference cuff measurements in many relevant individuals and during appreciable BP changes. Use of an ambulatory cuff device during daily life constitutes one option for building this database.
- Form factor: Conversion of smartphones into calibration-free BP monitors would improve hypertension awareness, whereas development of wearables, even with a cuff-calibrated method, is needed for hypotension surveillance in addition to hypertension diagnosis.
- Evaluation: Compelling evaluation of cuffless methods is a must (5, 96, 127). For example, machine learning models must show added value over baseline models in which the physiological measurement is excluded as input. IEEE Standard 1708 does exist for testing cuff-calibrated devices (see the sidebar titled First Standard for Cuffless BP Measurement Devices). While this standard includes invoking crucial intraindividual BP variations, the interventions required for inducing such changes are not delineated. Further consideration on standardized protocols is thus imperative. Since cuffless methods can uniquely provide many measurements over time, which could be averaged to mitigate error and intraindividual BP variations, even the error limits should be reconsidered (72). Ultimately, validation standards for cuffless methods must be developed and agreed upon for global use, feasible for wide application in many research centers, and able to accommodate the different types of devices.
- Wearables: Conception of solutions to overcome hydrostatic BP changes and motion is crucial for ambulatory monitoring and is especially challenging for finger-worn devices. However, the cuffless method should first be demonstrated in the absence of these confounding factors.

FIRST STANDARD FOR CUFFLESS BP MEASUREMENT DEVICES

In 2014, the Institute of Electrical and Electronics Engineers (IEEE) published the first standard for wearable cuffless blood pressure (BP) measurement devices (128). An amendment to this standard was published in 2019 (129). The salient points are as follows. A subject cohort of at least 85 individuals comprising low, normal, and high BP levels is required. The cuffless device is compared to reference manual auscultation BP measurements taken either sequentially or simultaneously. These comparisons are made in static conditions (*a*) immediately after individual user cuff calibration (according to the manufacturer instructions), (*b*) after inducing BP changes relative to the cuff BP level at calibration, and (*c*) before recalibration is recommended (according to manufacturer instructions). The BP changes may be induced in any way but must satisfy certain levels (e.g., at least 13.6% of the changes must be between 15 and 30 mm Hg and between −30 and −15 mm Hg). The pass requirements allow for a mean absolute error within 6 mm Hg for all cuffless BP measurements and within 7 mm Hg for the cuffless BP measurements after the BP change inducement.

Successful completion of these and other research directions could ultimately help reduce the global burden of elevated and low BP. We are optimistic about the feasibility of various cuff-calibrated devices for seamless tracking of BP changes in specific settings (e.g., nighttime), smartphone-based devices for ubiquitous BP monitoring, and finger rings for frequent BP measurement. We hope that this broad review helps advance cuffless BP measurement.

DISCLOSURE STATEMENT

R.M. has US National Institutes of Health (NIH) grants and patents on cuffless blood pressure measurement. Some of the patents have been licensed or optioned to Digitouch Health and Samsung Advanced Institute of Technology. G.S.S. has received honoraria for lectures at scientific symposia and for consulting services and research grants from several manufacturers of blood pressure monitoring technology, including Aktiia SA, Maisense Freescan, and Samsung Research America, Inc. A.P.A. is scientific advisor on the medical advisory board of CardieX.

ACKNOWLEDGMENTS

This work was supported in part by the NIH under grant HL146470.

LITERATURE CITED

1. GBD 2015 Mortal. Causes Death Collab. 2016. Global, regional, and national life expectancy, all-cause mortality, and cause-specific mortality for 249 causes of death, 1980–2015: a systematic analysis for the Global Burden of Disease Study 2015. *Lancet* 388:1459–544
2. Sessler, Daniel I, Saugel B. 2019. Beyond "failure to rescue": the time has come for continuous ward monitoring. *Br. J. Anaesth.* 122(3):304–6
3. Maheshwari K, Nathanson BH, Munson SH, Khangulov V, Stevens M, et al. 2018. The relationship between ICU hypotension and in-hospital mortality and morbidity in septic patients. *Intensive Care Med.* 44(6):857–67
4. Zenati MS, Billiar TR, Townsend RN, Peitzman AB, Harbrecht BG. 2002. A brief episode of hypotension increases mortality in critically ill trauma patients. *J. Trauma* 53(2):232–37
5. Tamura T. 2020. Regulation and approval of continuous non-invasive blood-pressure monitoring devices. In *MEDICON 2019: XV Mediterranean Conference on Medical and Biological Engineering and Computing*, ed. J Henriques, N Neves, P de Carvalho, pp. 1021–27. IFMBE Proc. 76. Cham, Switz.: Springer Nat.

6. Nachman D, Gepner Y, Goldstein N, Kabakov E, Ishay AB, et al. 2020. Comparing blood pressure measurements between a photoplethysmography-based and a standard cuff-based manometry device. *Sci. Rep.* 10:16116
7. Vybornova A, Polychronopoulou E, Wurzner-Ghajarzadeh A, Fallet S, Sola J, Wuerzner G. 2021. Blood pressure from the optical Aktiia bracelet: a 1-month validation study using an extended ISO81060-2 protocol adapted for a cuffless wrist device. *Blood Press. Monit.* 26(4):305–11
8. Ahn JH, Song J, Choi I, Youn J, Cho JW. 2021. Validation of blood pressure measurement using a smartwatch in patients with Parkinson's disease. *Front. Neurol.* 12:650929
9. Nair D, Tan S-Y, Gan H-W, Lim S-F, Yan J, et al. 2008. The use of ambulatory tonometric radial arterial wave capture to measure ambulatory blood pressure: the validation of a novel wrist-bound device in adults. *J. Hum. Hypertens.* 22(3):220–22
10. Mukkamala R, Hahn JO, Inan OT, Mestha LK, Kim CS, et al. 2015. Toward ubiquitous blood pressure monitoring via pulse transit time: theory and practice. *IEEE Trans. Biomed. Eng.* 62(8):1879–901
11. Sola J, Delgado-Gonzalo R, eds. 2019. *The Handbook of Cuffless Blood Pressure Monitoring: A Practical Guide for Clinicians, Researchers, and Engineers*. Cham, Switz.: Springer Nat.
12. Ding XR, Zhao N, Yang GZ, Pettigrew RI, Lo B, et al. 2016. Continuous blood pressure measurement from invasive to unobtrusive: celebration of 200th birth anniversary of Carl Ludwig. *IEEE J. Biomed. Heal. Inf.* 20(6):1455–65
13. Natarajan K, Yavarimanesh M, Wang W, Mukkamala R. 2021. Camera-based blood pressure monitoring. In *Contactless Vital Signs Monitoring*, ed. W Wang, X Wang, pp. 117–49. Oxford, UK: Elsevier
14. Mukkamala R, Hahn J-O, Chandrasekhar A. 2021. Photoplethysmography in non-invasive blood pressure monitoring. In *Photoplethysmography: Technology, Signal Analysis, and Applications*, ed. PA Kyriacou, J Allen. Oxford, UK: Elsevier
15. Buxi D, Redouté JM, Yuce MR. 2015. A survey on signals and systems in ambulatory blood pressure monitoring using pulse transit time. *Physiol. Meas.* 36(3):R1–26
16. Hosanee M, Chan G, Welykholowa K, Cooper R, Kyriacou PA, et al. 2020. Cuffless single-site photoplethysmography for blood pressure monitoring. *J. Clin. Med.* 9(3):723
17. Sharma M, Barbosa K, Ho V, Griggs D, Ghirmai T, et al. 2017. Cuff-less and continuous blood pressure monitoring: a methodological review. *Technologies* 5(2):21
18. Elgendi M, Fletcher R, Liang Y, Howard N, Lovell NH, et al. 2019. The use of photoplethysmography for assessing hypertension. *NPJ Digit. Med.* 2:60
19. Pandit JA, Lores E, Batlle D. 2020. Cuffless blood pressure monitoring: promises and challenges. *Clin. J. Am. Soc. Nephrol.* 15(10):1531–38
20. El-Hajj C, Kyriacou PA. 2020. A review of machine learning techniques in photoplethysmography for the non-invasive cuff-less measurement of blood pressure. *Biomed. Signal Process. Control.* 58:101870
21. O'Brien E, Fitzgerald D. 1994. The history of blood pressure measurement. *J. Hum. Hypertens.* 8:73–84
22. Marino PL. 2007. *The ICU Book*. Philadelphia: Lippincott Williams & Wilkins. 3rd ed.
23. Wesseling KH, Jansen JRC, Settels JJ, Schreuder JJ. 1993. Computation of aortic flow from pressure in humans using a nonlinear, three-element model. *J. Appl. Physiol.* 74(5):2566–73
24. Mukkamala R, Xu D. 2010. Continuous and less invasive central hemodynamic monitoring by blood pressure waveform analysis. *Am. J. Physiol. Heart Circ. Physiol.* 299(3):584–99
25. Perloff D, Grim C, Flack J, Frohlich ED. 1993. Human blood pressure determination by sphygmomanometry. *Circulation* 88:2460–70
26. Ng K-G, Small CF. 1994. Survey of automated noninvasive blood pressure monitors. *J. Clin. Eng.* 19(6):452–75
27. Forouzanfar M, Dajani HR, Groza VZ, Bolic M, Rajan S, Batkin I. 2015. Oscillometric blood pressure estimation: past, present, and future. *IEEE Rev. Biomed. Eng.* 8:44–63
28. Drzewiecki G, Hood R, Apple H. 1994. Theory of the oscillometric maximum and the systolic and diastolic detection ratios. *Ann. Biomed. Eng.* 22(1):88–96
29. Ramsey M. 1979. Noninvasive automatic determination of mean arterial pressure. *Med. Biol. Eng. Comput.* 17(1):11–18
30. Geddes LA, Voelz M, Combs C, Reiner D, Babbs CE. 1982. Characterization of the oscillometric method for measuring indirect blood pressure. *Ann. Biomed. Eng.* 10:271–80

31. Penáz J. 1992. Criteria for set point estimation in the volume clamp method of blood pressure measurement. *Physiol. Res.* 41(1):5–10
32. Imholz BPM, Wieling W, Van Montfrans GA, Wesseling KH. 1998. Fifteen years experience with finger arterial pressure monitoring: assessment of the technology. *Cardiovasc. Res.* 38(3):605–16
33. Fortin J, Marte W, Grüllenberger R, Hacker A, Habenbacher W, et al. 2006. Continuous non-invasive blood pressure monitoring using concentrically interlocking control loops. *Comput. Biol. Med.* 36(9):941–57
34. Matsumura K, Yamakoshi T, Rolfe P, Yamakoshi KI. 2017. Advanced volume-compensation method for indirect finger arterial pressure determination: comparison with brachial sphygmomanometry. *IEEE Trans. Biomed. Eng.* 64(5):1131–37
35. Pressman GL, Newgard PM. 1963. A transducer for the continuous external measurement of arterial blood pressure. *IEEE Trans. Bio-Med. Electron.* 10(2):73–81
36. Eckerle JS. 2006. Tonometry, arterial. In *Encyclopedia of Medical Devices and Instrumentation*, ed. JG Webster, pp. 402–10. New York: Wiley
37. Drzewiecki GM, Melbin J, Noordergraaf A. 1983. Arterial tonometry: review and analysis. *J. Biomech.* 16(2):141–52
38. Lewington S, Clarke R, Qizilbash N, Peto R, Collins R. 2002. Age-specific relevance of usual blood pressure to vascular mortality: a meta-analysis of individual data for one million adults in 61 prospective studies. *Lancet* 360(9349):1903–13
39. Picone DS, Schultz MG, Otahal P, Aakhus S, Al-Jumaily AM, et al. 2017. Accuracy of cuff-measured blood pressure: systematic reviews and meta-analyses. *J. Am. Coll. Cardiol.* 70(5):572–86
40. Stergiou GS, Alpert BS, Mieke S, Wang J, O'Brien E. 2018. Validation protocols for blood pressure measuring devices in the 21st century. *J. Clin. Hypertens.* 20:1096–99
41. Stergiou GS, Alpert B, Mieke S, Asmar R, Atkins N, et al. 2018. A universal standard for the validation of blood pressure measuring devices: Association for the Advancement of Medical Instrumentation/European Society of Hypertension/International Organization for Standardization (AAMI/ESH/ISO) collaboration statement. *Hypertension* 71(3):368–74
42. Nichols WW, O'Rourke MF, Vlachopoulos C. 2011. *McDonald's Blood Flow in Arteries: Theoretical, Experimental, and Clinical Principles*. London: Hodder Arnold
43. Karamanoglu M, O'Rourke MF, Avolio AP, Kelly RP. 1993. An analysis of the relationship between central aortic and peripheral upper limb pressure waves in man. *Eur. Heart J.* 14(2):160–67
44. Gizdulich P, Prentza A, Wesseling KH. 1997. Models of brachial to finger pulse wave distortion and pressure decrement. *Cardiovasc. Res.* 33(3):698–705
45. Giorgini P, Weder AB, Jackson EA, Brook RD. 2014. A review of blood pressure measurement protocols among hypertension trials: implications for "evidence-based" clinical practice. *J. Am. Soc. Hypertens.* 8(9):670–76
46. Chow CK, Teo KK, Rangarajan S, Islam S, Gupta R, et al. 2013. Prevalence, awareness, treatment, and control of hypertension in rural and urban communities in high-, middle-, and low-income countries. *JAMA* 310(9):959–68
47. Pickering TG, Phil D, Shimbo D, Haas D. 2006. Ambulatory blood-pressure monitoring. *N. Engl. J. Med.* 354(22):2368–74
48. Rosner B, Polk BF. 1983. Predictive values of routine blood pressure measurements in screening for hypertension. *Am. J. Epidemiol.* 117(4):429–42
49. Taira D, Sentell T, Albright C, Lansidell D, Nakagawa K, et al. 2017. Insights in public health: ambulatory blood pressure monitoring: underuse in clinical practice in Hawai'i. *Hawai'i J. Med. Public Health* 76(11):314–17
50. Asayama K, Fujiwara T, Hoshide S, Ohkubo T, Kario K, et al. 2019. Nocturnal blood pressure measured by home devices: evidence and perspective for clinical application. *J. Hypertens.* 37(5):905–16
51. Agarwal R, Bills JE, Hecht TJW, Light RP. 2011. Role of home blood pressure monitoring in overcoming therapeutic inertia and improving hypertension control: a systematic review and meta-analysis. *Hypertension* 57:29–38
52. Zheng YL, Ding XR, Poon CCY, Lo BPL, Zhang H, et al. 2014. Unobtrusive sensing and wearable devices for health informatics. *IEEE Trans. Biomed. Eng.* 61(5):1538–54

53. Reisner A, Shaltis PA, McCombie D, Asada HH. 2008. Utility of the photoplethysmogram in circulatory monitoring. *Anesthesiology* 108(5):950–58
54. Allen J. 2007. Photoplethysmography and its application in clinical physiological measurement. *Physiol. Meas.* 28(3):R1–39
55. Tamura T, Maeda Y, Sekine M, Yoshida M. 2014. Wearable photoplethysmographic sensors—past and present. *Electron* 3(2):282–302
56. Gill RW. 1985. Measurement of blood flow by ultrasound: accuracy and sources of error. *Ultrasound Med. Biol.* 11(4):625–41
57. Bera TK. 2014. Bioelectrical impedance methods for noninvasive health monitoring: a review. *J. Med. Eng.* 2014:381251
58. Patterson RP. 1989. Fundamentals of impedance cardiography. *IEEE Eng. Med. Biol. Mag.* 8(1):35–38
59. Inan OT, Migeotte PF, Park KS, Etemadi M, Tavakolian K, et al. 2015. Ballistocardiography and seismocardiography: a review of recent advances. *IEEE J. Biomed. Heal. Inf.* 19(4):1414–27
60. Kim CS, Ober SL, McMurtry MS, Finegan BA, Inan OT, et al. 2016. Ballistocardiogram: mechanism and potential for unobtrusive cardiovascular health monitoring. *Sci. Rep.* 6:31297
61. Jonathan E, Leahy M. 2010. Investigating a smartphone imaging unit for photoplethysmography. *Physiol. Meas.* 31(11):N79–83
62. Verkruysse W, Svaasand LO, Nelson JS. 2008. Remote plethysmographic imaging using ambient light. *Opt. Express* 16(26):21434
63. Balakrishnan G, Durand F, Guttag J. 2013. Detecting pulse from head motions in video. In *2013 IEEE Conference on Computer Vision and Pattern Recognition*, pp. 3430–37. Los Alamitos, CA: IEEE Comput. Soc.
64. Landreani F, Caiani EG. 2017. Smartphone accelerometers for the detection of heart rate. *Expert Rev. Med. Devices* 14(12):935–48
65. Dunn J, Runge R, Snyder M. 2018. Wearables and the medical revolution. *Pers. Med.* 15(5):429–48
66. Chung HU, Rwei AY, Hourlier-Fargette A, Xu S, Lee KH, et al. 2020. Skin-interfaced biosensors for advanced wireless physiological monitoring in neonatal and pediatric intensive-care units. *Nat. Med.* 26(3):418–29
67. Schwartz G, Tee BCK, Mei J, Appleton AL, Kim DH, et al. 2013. Flexible polymer transistors with high pressure sensitivity for application in electronic skin and health monitoring. *Nat. Commun.* 4:1859
68. Wang C, Li X, Hu H, Zhang L, Huang Z, et al. 2018. Monitoring of the central blood pressure waveform via a conformal ultrasonic device. *Nat. Biomed. Eng.* 2(9):687–95
69. Ha T, Tran J, Liu S, Jang H, Jeong H, et al. 2019. A chest-laminated ultrathin and stretchable e-tattoo for the measurement of electrocardiogram, seismocardiogram, and cardiac time intervals. *Adv. Sci.* 6:1900290
70. Bramwell JC, Hill AV. 1922. The velocity of pulse wave in man. *Proc. R. Soc. B* 93(652):298–306
71. Yavarimanesh M, Chandrasekhar A, Hahn J-O, Mukkamala R. 2019. Commentary: relation between blood pressure and pulse wave velocity for human arteries. *Front. Physiol.* 10:1170
72. Mukkamala R, Hahn JO. 2018. Toward ubiquitous blood pressure monitoring via pulse transit time: predictions on maximum calibration period and acceptable error limits. *IEEE Trans. Biomed. Eng.* 65(6):1410–20
73. Gao M, Olivier NB, Mukkamala R. 2016. Comparison of noninvasive pulse transit time estimates as markers of blood pressure using invasive pulse transit time measurements as a reference. *Physiol. Rep.* 4(10):e12768
74. Chiu YC, Arand PW, Shroff SG, Feldman T, Carroll JD. 1991. Determination of pulse wave velocities with computerized algorithms. *Am. Heart J.* 121(5):1460–70
75. Chandrasekhar A, Yavarimanesh M, Natarajan K, Hahn JO, Mukkamala R. 2020. PPG sensor contact pressure should be taken into account for cuff-less blood pressure measurement. *IEEE Trans. Biomed. Eng.* 67(11):3134–40
76. Mukkamala R, Hahn JO. 2019. Initialization of pulse transit time-based blood pressure monitors. In *The Handbook of Cuffless Blood Pressure Monitoring: A Practical Guide for Clinicians, Researchers, and Engineers*, ed. J Sola, R Delgado-Gonzolo, pp. 163–90. Cham, Switz.: Springer Nat.

77. Gavish B, Ben-Dov IZ, Bursztyn M. 2008. Linear relationship between systolic and diastolic blood pressure monitored over 24 h: assessment and correlates. *J. Hypertens.* 26(2):199–209
78. Master AM, Lasser RP. 1965. The relationship of pulse pressure and diastolic pressure to systolic pressure in healthy subjects, 20–94 years of age. *Am. Heart J.* 70(2):163–71
79. McCombie DB, Shaltis PA, Reisner AT, Asada HH. 2007. Adaptive hydrostatic blood pressure calibration: development of a wearable, autonomous pulse wave velocity blood pressure monitor. In *29th Annual International Conference of the IEEE Engineering in Medicine and Biology Society*, pp. 370–73. Piscataway, NJ: IEEE
80. Butlin M, Shirbani F, Barin E, Tan I, Spronck B, Avolio AP. 2018. Cuffless estimation of blood pressure: importance of variability in blood pressure dependence of arterial stiffness across individuals and measurement sites. *IEEE Trans. Biomed. Eng.* 65(11):2377–83
81. Chen Y, Wen C, Tao G, Bi M, Li G. 2009. Continuous and noninvasive blood pressure measurement: a novel modeling methodology of the relationship between blood pressure and pulse wave velocity. *Ann. Biomed. Eng.* 37(11):2222–33
82. Payne RA, Symeonides CN, Webb DJ, J Maxwell SR. 2006. Pulse transit time measured from the ECG: an unreliable marker of beat-to-beat blood pressure. *J. Appl. Physiol.* 100:136–41
83. Liang Y, Abbott D, Howard N, Lim K, Ward R, Elgendi M. 2019. How effective is pulse arrival time for evaluating blood pressure? Challenges and recommendations from a study using the MIMIC database. *J. Clin. Med.* 8(3):337
84. Yoon YZ, Kang JM, Kwon Y, Park S, Noh S, et al. 2018. Cuff-less blood pressure estimation using pulse waveform analysis and pulse arrival time. *IEEE J. Biomed. Heal. Inf.* 22(4):1068–74
85. Sharwood-Smith G, Bruce J, Drummond G. 2006. Assessment of pulse transit time to indicate cardiovascular changes during obstetric spinal anaesthesia. *Br. J. Anaesth.* 96(1):100–5
86. Lee J, Yang S, Lee S, Kim HC. 2019. Analysis of pulse arrival time as an indicator of blood pressure in a large surgical biosignal database: recommendations for developing ubiquitous blood pressure monitoring methods. *J. Clin. Med.* 8(11):1773
87. Kim CS, Carek AM, Inan OT, Mukkamala R, Hahn JO. 2018. Ballistocardiogram-based approach to cuffless blood pressure monitoring: proof of concept and potential challenges. *IEEE Trans. Biomed. Eng.* 65(11):2384–91
88. Block RC, Yavarimanesh M, Natarajan K, Carek A, Mousavi A, et al. 2020. Conventional pulse transit times as markers of blood pressure changes in humans. *Sci. Rep.* 10:16373
89. Di Rienzo M, Avolio A, Rizzo G, Isilay Zeybek ZM, Cucugliato L. 2022. Multi-site pulse transit times, beat-to-beat blood pressure, and isovolumic contraction time at rest and under stressors. *IEEE J. Biomed. Health Inform.* 26(2):561–71
90. Flügge W. 1975. *Viscoelasticity*. Heidelberg, Ger.: Springer-Verlag
91. Natarajan K, Block RC, Yavarimanesh M, Chandrasekhar A, Mestha LK, et al. 2022. Photoplethysmography fast upstroke time intervals can be useful features for cuff-less measurement of blood pressure changes in humans. *IEEE Trans. Biomed. Eng.* 69(1):53–62
92. Fortin J, Rogge DE, Fellner C, Flotzinger D, Grond J, et al. 2021. A novel art of continuous noninvasive blood pressure measurement. *Nat. Commun.* 12:1387
93. Elgendi M. 2012. On the analysis of fingertip photoplethysmogram signals. *Curr. Cardiol. Rev.* 8(1):14–25
94. Addison PS. 2016. Slope transit time (STT): a pulse transit time proxy requiring only a single signal fiducial point. *IEEE Trans. Biomed. Eng.* 63(11):2441–44
95. Baruch MC, Warburton DER, Bredin SSD, Cote A, Gerdt DW, Adkins CM. 2011. Pulse decomposition analysis of the digital arterial pulse during hemorrhage simulation. *Nonlinear Biomed. Phys.* 5:1
96. Mukkamala R, Yavarimanesh M, Natarajan K, Hahn J-O, Kyriakoulis KG, et al. 2021. Evaluation of the accuracy of cuffless blood pressure measurement devices: challenges and proposals. *Hypertension* 78:1161–67
97. Xing X, Ma Z, Zhang M, Zhou Y, Dong W, Song M. 2019. An unobtrusive and calibration-free blood pressure estimation method using photoplethysmography and biometrics. *Sci. Rep.* 9:8611
98. Ruiz-Rodríguez JC, Ruiz-Sanmartín A, Ribas V, Caballero J, García-Roche A, et al. 2013. Innovative continuous non-invasive cuffless blood pressure monitoring based on photoplethysmography technology. *Intensive Care Med.* 39(9):1618–25

99. Xing X, Ma Z, Zhang M, Gao X, Li Y, et al. 2020. Robust blood pressure estimation from finger photoplethysmography using age-dependent linear models. *Physiol. Meas.* 41:025007
100. Radha M, De Groot K, Rajani N, Wong CCP, Kobold N, et al. 2019. Estimating blood pressure trends and the nocturnal dip from photoplethysmography. *Physiol. Meas.* 40:025006
101. Mukkamala R. 2019. Blood pressure with a click of a camera? *Circ. Cardiovasc. Imaging* 12(8):e009531
102. Viola P, Jones M. 2001. Rapid object detection using a boosted cascade of simple features. In *2001 IEEE Computer Society Conference on Computer Vision and Pattern Recognition: CVPR 2001*, pp. I-511–18. Los Alamitos, CA: IEEE Comput. Soc.
103. Wang W, Den Brinker AC, Stuijk S, De Haan G. 2017. Algorithmic principles of remote PPG. *IEEE Trans. Biomed. Eng.* 64(7):1479–91
104. Bouguet J-Y. 2001. *Pyramidal implementation of the affine Lucas Kanade feature tracker description of the algorithm*. Rep., Intel. Corp., Santa Clara, CA
105. Jeong IC, Finkelstein J. 2016. Introducing contactless blood pressure assessment using a high speed video camera. *J. Med. Syst.* 40(4):77
106. Luo H, Yang D, Barszczyk A, Vempala N, Wei J, et al. 2019. Smartphone-based blood pressure measurement using transdermal optical imaging technology. *Circ. Cardiovasc. Imaging* 12(8):e008857
107. Poplin R, Varadarajan AV, Blumer K, Liu Y, McConnell MV, et al. 2018. Prediction of cardiovascular risk factors from retinal fundus photographs via deep learning. *Nat. Biomed. Eng.* 2(3):158–64
108. Shaltis PA, Reisner AT, Asada HH. 2008. Cuffless blood pressure monitoring using hydrostatic pressure changes. *IEEE Trans. Biomed. Eng.* 55(6):1775–77
109. Chandrasekhar A, Kim CS, Naji M, Natarajan K, Hahn JO, Mukkamala R. 2018. Smartphone-based blood pressure monitoring via the oscillometric finger-pressing method. *Sci. Transl. Med.* 10(431). **https://doi.org/10.1126/scitranslmed.aap8674**
110. Chandrasekhar A, Natarajan K, Yavarimanesh M, Mukkamala R. 2018. An iPhone application for blood pressure monitoring via the oscillometric finger pressing method. *Sci. Rep.* 8:13136
111. Chandrasekhar A, Yavarimanesh M, Hahn JO, Sung SH, Chen CH, et al. 2019. Formulas to explain popular oscillometric blood pressure estimation algorithms. *Front. Physiol.* 10:1415
112. Liu J, Cheng HM, Chen CH, Sung SH, Hahn JO, Mukkamala R. 2017. Patient-specific oscillometric blood pressure measurement: validation for accuracy and repeatability. *IEEE J. Transl. Eng. Heal. Med.* 5:1900110
113. Babbs CF. 2012. Oscillometric measurement of systolic and diastolic blood pressures validated in a physiologic mathematical model. *Biomed. Eng. Online* 11:56
114. Panula T, Koivisto T, Pänkäälä M, Niiranen T, Kantola I, Kaisti M. 2020. An instrument for measuring blood pressure and assessing cardiovascular health from the fingertip. *Biosens. Bioelectron.* 167:112483
115. Kario K, Shimbo D, Tomitani N, Kanegae H, Schwartz JE, Williams B. 2020. The first study comparing a wearable watch-type blood pressure monitor with a conventional ambulatory blood pressure monitor on in-office and out-of-office settings. *J. Clin. Hypertens.* 22(2):135–41
116. Beulen BWAMM, Bijnens N, Koutsouridis GG, Brands PJ, Rutten MCM, van de Vosse FN. 2011. Toward noninvasive blood pressure assessment in arteries by using ultrasound. *Ultrasound Med. Biol.* 37(5):788–97
117. Gao M, Cheng HM, Sung SH, Chen CH, Olivier NB, Mukkamala R. 2017. Estimation of pulse transit time as a function of blood pressure using a nonlinear arterial tube-load model. *IEEE Trans. Biomed. Eng.* 64(7):1524–34
118. Seo J, Pietrangelo SJ, Lee HS, Sodini CG. 2015. Noninvasive arterial blood pressure waveform monitoring using two-element ultrasound system. *IEEE Trans. Ultrason. Ferroelectr. Freq. Control.* 62(4):776–84
119. Vappou J, Luo J, Okajima K, Di Tullio M, Konofagou EE. 2011. Non-invasive measurement of local pulse pressure by pulse wave-based ultrasound manometry (PWUM). *Physiol. Meas.* 32(10):1653–62
120. Joseph J, Nabeel PM, Shah MI, Sivaprakasam M. 2018. Arterial compliance probe for cuffless evaluation of carotid pulse pressure. *PLOS ONE* 13(8):e0202480
121. Vlachopoulos C, Aznaouridis K, O'Rourke MF, Safar ME, Baou K, Stefanadis C. 2010. Prediction of cardiovascular events and all-cause mortality with central haemodynamics: a systematic review and meta-analysis. *Eur. Heart J.* 31(15):1865–71

122. Seo J, Lee HS, Sodini CG. 2021. Non-invasive evaluation of a carotid arterial pressure waveform using motion-tolerant ultrasound measurements during the Valsalva maneuver. *IEEE J. Biomed. Heal. Inf.* 25(1):163–74
123. Nabeel PM, Joseph J, Karthik S, Sivaprakasam M, Chenniappan M. 2018. Bi-modal arterial compliance probe for calibration-free cuffless blood pressure estimation. *IEEE Trans. Biomed. Eng.* 65(11):2392–404
124. Liu J, Hahn JO, Mukkamala R. 2013. An initial step towards improving the accuracy of the oscillometric blood pressure measurement. In *35th Annual International Conference of the IEEE Engineering in Medicine and Biology Society (EMBC)*, pp. 4082–85. Piscataway, NJ: IEEE
125. Zakrzewski AM, Huang AY, Zubajlo R, Anthony BW. 2018. Real-time blood pressure estimation from force-measured ultrasound. *IEEE Trans. Biomed. Eng.* 65(11):2405–16
126. Johnson AEW, Pollard TJ, Shen L, Lehman LWH, Feng M, et al. 2016. MIMIC-III, a freely accessible critical care database. *Sci. Data* 3:160035
127. van Helmond N, Martin SS, Plante TB. 2020. Is cuffless blood pressure measurement already here? *J. Hypertens.* 38(4):774–75
128. IEEE. 2014. *IEEE Standard for Wearable Cuffless Blood Pressure Measuring Devices*. New York: IEEE. 38 pp.
129. IEEE. 2019. *IEEE Standard for Wearable, Cuffless Blood Pressure Measuring Devices - Amendment 1*. New York: IEEE. 35 pp.